Computerized Medical Imaging and Graphics xxx (2016) xxx–xxx

Contents lists available at ScienceDirect

Computerized Medical Imaging and Graphics

journal homepage: www.elsevier.com/locate/compmedimag

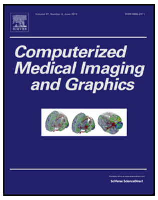

Talar dome detection and its geometric approximation in CT: Sphere, cylinder or bi-truncated cone?

Junbin Huang[a,b,1], He Liu[c,1], Defeng Wang[a,b,d], James F. Griffith[a], Lin Shi[e,f,*]

[a] *Department of Imaging and Interventional Radiology, The Chinese University of Hong Kong, Shatin, NT, Hong Kong*
[b] *Research Center for Medical Image Computing, The Chinese University of Hong Kong, Shatin, NT, Hong Kong*
[c] *Department of Interventional Neuroradiology, Beijing Chaoyang Hospital, Capital Medical University, Beijing, China*
[d] *Shenzhen Research Institute, The Chinese University of Hong Kong, Shenzhen, China*
[e] *Department of Medicine and Therapeutics, The Chinese University of Hong Kong, Shatin, NT, Hong Kong*
[f] *Chow Yuk Ho Center of Innovative Technology for Medicine, The Chinese University of Hong Kong, Shatin, NT, Hong Kong*

ARTICLE INFO

Article history:
Received 1 February 2016
Received in revised form 17 May 2016
Accepted 4 June 2016

Keywords:
Computed tomography
Talar dome
Shape quantification
Least-square

ABSTRACT

Objective: The purpose of our study is to give a relatively objective definition of talar dome and its shape approximations to sphere (SPH), cylinder (CLD) and bi-truncated cone (BTC).

Materials and methods: The “talar dome” is well-defined with the improved Dijkstra’s algorithm, considering the Euclidean distance and surface curvature. The geometric similarity between talar dome and ideal shapes, namely SPH, CLD and BTC, is quantified. 50 unilateral CT datasets from 50 subjects with no pathological morphometry of tali were included in the experiments and statistical analyses were carried out based on the approximation error.

Results: The similarity between talar dome and BTC was more prominent, with smaller mean, standard deviation, maximum and median of the approximation error (0.36 ± 0.07 mm, 0.32 ± 0.06 mm, 2.24 ± 0.47 mm and 0.28 ± 0.06 mm) compare with fitting to SPH and CLD. In addition, there were significant differences between the fitting error of each pair of models in terms of the 4 measurements (p-values < 0.05). The linear regression analyses demonstrated high correlation between CLD and BTC approximations ($R^2 = 0.55$ for median, $R^2 > 0.7$ for others). Color maps representing fitting error indicated that fitting error mainly occurred on the marginal regions of talar dome for SPH and CLD fittings, while that of BTC was small for the whole talar dome.

Conclusion: The successful restoration of ankle functions in displacement surgery highly depends on the comprehensive understanding of the talus. The talar dome surface could be well-defined in a computational way and compared to SPH and CLD, the talar dome reflects outstanding similarity with BTC.

1. Introduction

The human ankle is a flexible structure with multiple movement abilities including internal/external rotation, dorsiflexion/plantar flexion and inversion/eversion (Koh et al., 2004). Orthopaedic ankle-related surgery is one of the widely-used treatments for osteochondral lesions of the talus whose aim is the reproduction of the physiological functions of ankle joint. This restoration is particularly important for ligaments tensioning (Leardini, 2001). The shapes of the implanted material should be compatible with the geometry of the ligamentous structures. Unfortunately, the success rate of this operation is usually lowered by the mismatch of implanted compound with the natural morphometry of the ankle (Valderrabano et al., 2009). Failure to restore the conventional movements of ankle and the deficiency of talar dome morphometry knowledge can be a bottle-neck in such operations. Due to the complicated 3D configuration of talus, improper bone displacement of the ankle joint will cause deterioration and poor treatment result even with slight difference between natural and implanted talus (Koh et al., 2004; Valderrabano et al., 2009).

Literature on the morphometry analysis of talus is relatively limited. As X-ray pictures are widely used on conventional osseous disease diagnosis, Tochigi et al. designed an experiment to evaluate the sensitivity of ankle positioning on ankle geometry measurement, in which they found the T-T ratio seemed to have a more reasonable tolerance than P-T (Tochigi et al., 2006). Stagni et al.

---

* Corresponding author at: Department of Medicine and Therapeutics, The Chinese University of Hong Kong, Prince of Wales Hospital, Shatin, NT, Hong Kong.
E-mail address: shilin@cuhk.edu.hk (L. Shi).

[1] Both authors contributed equally to this work.

http://dx.doi.org/10.1016/j.compmedimag.2016.06.002
0895-6111/

Please cite this article in press as: Huang, J., et al., Talar dome detection and its geometric approximation in CT: Sphere, cylinder or bi-truncated cone? Comput Med Imaging Graph (2016), http://dx.doi.org/10.1016/j.compmedimag.2016.06.002

used up to 12 measurements for ankle morphometry evaluation, where a steel sphere was necessary to be stuck into the ankle (Stagni et al., 2005). CT images were also applied in some other publications. Some measurements based on CT were also obtained from the sagittal, coronal and axial views. However, the geometry parameters were measured with software or manually, which was time-consuming for large data number (Wiewiorski et al., 2012). Although CT data were used in those studies, its advantage in 3D reconstruction was not reflected as the researchers made measurements on the 2D views.

Examinations using conventional X-ray can only provide 2D images and measurements based on these images will give different results with different scanning position. Compared with 2D-based radiographic images, 3D-based modalities like CT or MRI present a better performance on organs/tissues visualization, which makes it feasible to analyze complex geometry of talus. However, the definition of “talar dome” is ambiguous. Although it had been proposed by Inman et al. since 1976 that the shape of talar dome should be conical rather than cylindrical (Inman, 1991), no 3D quantification is presented to support such an opinion. An objective method to define the talar dome surface should be an effective way to facilitate the analysis of talus based on 3D surface.

The purpose of this study aims to give a more clearly definition for “talar dome” and a better understanding of this structure. The rest of this paper will propose a method for the detection of talar dome with small interactions by considering the curvature information of the talar surface and the distance information between neighboring landmarks. Then the talar dome is best fitted to sphere, cylinder and bi-truncated cone, respectively. Statistical analyses are achieved based on the fitting outcomes and the results will be given.

2. Materials and methods

2.1. Data acquisition

In this study, a group of 50 ankle CT scans (31 males, 38.19 ± 17.81 years, age range, 12–88 years; 19 females, 44.56 ± 20.49 years, age range, 11–90 years) was prospectively obtained to quantify the shape of talar dome. All of the participants were chosen from those who accepted CT examinations of the lower extremities, in which the intact tali were included in the field of view. At the time of scanning, individuals reflected no abnormal and pathologic characters of the tali. CT examination was performed on a 64-slice multi-detector CT scanner (LightSpeed Ultra, GE Healthcare, Milwaukee, WI, USA) with a 50 cm scan field of view, a 0.625 mm thick slice acquisition with no spacing, 120 kVp, X-ray tube current 300 mA, 0.6 s scan time, and imaging reconstruction using a standard reconstruction algorithm for bone.

2.2. 3D surface reconstruction

For the reconstruction of talar surface, the talus was first separated from other indifferent bones and soft tissues using CT images. After conventional pre-processing, i.e., denoising, image enhancement (Gonzalez and Woods, 2007), the talus was extracted in a semi-automatic manner using ITK-SNAP (http://www.itksnap.org/). The objects with high intensity were first segmented with thresholding method. Then the voxels connecting talus with other uninterested bone structures were eliminated, after which the talar component was extracted automatically. After filling the edges of talus, the hole filling operation was achieve to obtain the final segmentation result. For each data, the processing time is about 20 min. The marching cubes algorithm (Lorensen and Cline, 1987) was then used to reconstruct the 3D surface of talus after applying the 3D Gaussian smoothing filter on the segmented binary images.

2.3. Detection of talar dome surface

For shape quantification and analysis, the surface of talar dome had to be separated from other surfaces of the talus. Because of its distinctive difference from the glenoid, the incremental watershed algorithm we previously proposed (Shi et al., 2013) is not appropriate for the detection of talar dome surface, as the transitional regions between talar dome and other surfaces are less prominent than that between glenoid and other surfaces. In this study, a novel combination of Euclidean distance and surface curvature was applied to extract talar dome with small interactions. The contour separating talar dome and other surfaces was defined using

$$\begin{aligned} Path_{[a,b]} &= arg\min \sum_{i=1}^{n-1} \frac{2D(i,i+1)}{Curv(i)+Curv(i+1)}, [a,b] \\ &= [p_1,p_2],[p_2,p_3],[p_3,p_4],[p_4,p_1], \end{aligned}$$

where $Path_{[a,b]}$ is the path from a to b, n is the number of edges of the triangulations on $Path_{[a,b]}$, $D(i,i+1)$ is the Euclidean distance between vertices i and $i+1$, $Curv(i)$ is the curvature of i. $i=1$ indicates the source vertex (i.e., a) while $i=n$ is for the terminal vertex (i.e., b). As 4 landmarks p_1, p_2, p_3 and p_4, which are located on the four corners of talar dome determined by experienced radiologist, are selected in our experiments, the definition of $[a,b]$ is as the formula indicates.

The objective function for talar dome surface detection is an application of the Dijkstra’s algorithm, for which the optimization can be achieved with the algorithm (Dijkstra, 1959). The difference between our formula and the original algorithm is the definition of the edge weights. Based on the assumption that the curvatures between neighboring surfaces should be larger than those inside surfaces, the function above takes a balance between curvatures and length of the path. It aims to find the path on which the curvatures of the vertices are large, while the distance between the source and terminal vertex is small (Fig. 1).

2.4. Shape approximation

The talar dome acquired was fitted to three common geometries: sphere, cylinder and bi-truncated cone. The approximation to a sphere was achieved with a commonly used least-square method (Leon, 2009). For the cylinder and bi-truncated cone fittings, the minimal bounding box (Gonzalez and Woods, 2007) of the surface was firstly obtained and the coordinates of the vertices were transformed, using the three principal edges of the box as the directions of new coordinate axes. The surface was firstly fitted to the cylinder, using the center of the fitted sphere as an estimated point on the axis of the cylinder. For the bi-truncated fitting, the dataset was firstly divided into two parts using the anterior-superior plane which is parallel with the lateral surface of the bounding box as well as divding the minimal bounding box into two parts with same volume (Fig. 2). Respectively, the two datasets were then fitted to truncated cones. The optimization was achieved using the LSGE MATLAB software package based on least-square optimization (http://www.eurometros.org/metros/packages/lsge/) (Fig. 3).

2.5. Statistical analysis

The Euclidean distances between vertices on the talar dome surface and the ideal geometries, namely sphere (SPH), cylinder (CLD) and bi-truncated cone (BTC), were calculated. For each data, the mean, standard deviation (STD), maximum and median of the distances were calculated and presented as mean ± standard deviation. The paired Student’s t-test was applied to test for the statistical significance of fitting results between each pair of models (i.e., SPH

Please cite this article in press as: Huang, J., et al., Talar dome detection and its geometric approximation in CT: Sphere, cylinder or bi-truncated cone? Comput Med Imaging Graph (2016), http://dx.doi.org/10.1016/j.compmedimag.2016.06.002